LOW-ENERGY ESCAPE FROM THE SUN-EARTH L_2 HALO ORBIT UTILIZING UNSTABLE MANIFOLDS AND LUNAR GRAVITY ASSIST

Chen, Hongru
Department of Aeronautics and Astronautics, Kyushu University : Ph.D. Candidate

Kawakatsu, Yasuhiro
Department of Space Flight Systems, ISAS/JAXA : Associate Professor

Hanada, Toshiya
Department of Aeronautics and Astronautics, Kyushu University : Professor

出版情報：Advances in the astronautical sciences. 152, pp.3679-3691, 2014. Univelt Inc.
バージョン：
権利関係：

AAS 14-468

LOW-ENERGY ESCAPE FROM THE SUN-EARTH L2 HALO ORBIT UTILIZING UNSTABLE MANIFOLDS AND LUNAR GRAVITY ASSIST

Hongru Chen,[*] Yasuhiro Kawakatsu[†] and Toshiya Hanada[‡]

The paper investigates the escape strategy using the unstable manifolds of the Sun-Earth L_2 halo orbit and lunar gravity assist. There are four cases of intersection of the manifold tubes associated with halo orbits and the orbit of the Moon. The four intersections have different V_∞ with respect to the Moon. The corresponding lunar gravity assists can result in a range of escape trajectories, granting choices for the extended mission of halo orbits. In order to satisfy the lunar encounter requirements, the strategy and ΔV costs of phasing maneuvers are presented as well.

INTRODUCTION

Low-energy escape trajectories have been intensively studied, increasing the possibility and flexibility of interplanetary missions. Escaping from the Earth system with minimum fuel cost is usually the primary task mission designers should consider. The fuel saving will contribute to the increase of payload mass. A traditional approach is using gravity assists to lift up the energy of a spacecraft. Utilizing lunar gravity assist to escape from the Earth has been demonstrated by a number of mission designs.[1-3] A single or double lunar swingbys can propel the spacecraft from a captured C_3 of -1.5km^2/s^2 to an escape C_3 of 2km^2/s^2. An escape C3 of 2km^2/s^2 can be efficiently utilized with the solar electric Earth gravity assist, making going to the targets as far as the Jupiter possible (See Reference 4).

The Lagrange points of the 3-body problem offer many new orbits and applications. There have been many successful missions around the Sun-Earth liberation points L_1 and L_2, e.g. the famous ISEE-3 and Genesis. Giving a small ΔV, the spacecraft in a halo orbit about the libration point will depart away along an unstable manifold and thereafter escape from the Earth or other gravity systems of interest. On the contrary, a spacecraft can asymptotically inject into a halo orbit along its stable manifolds. The manifold structure prescribes the phase space, providing the design strategies for orbit transfers. There have been proposals exploiting the Lagrange point dynamics for low energy transfers.[5-9]

---

[*] Ph.D. Candidate, Department of Aeronautics and Astronautics, Kyushu University, 744 Motooka, Nishi-ku, Fukuoka 819-0395, Japan.
[†] Associate Professor, Department of Space Flight Systems, ISAS/JAXA, 3-1-1 Yoshinodai, Sagamihara 252-5210, Japan.
[‡] Professor, Department of Aeronautics and Astronautics, Kyushu University, 744 Motooka, Nishi-ku, Fukuoka 819-0395, Japan.

As an attempt of making use of both advantages, the present study investigates the combination of manifold dynamics and lunar gravity assist for low-energy escape. The JAXA mission DESTINY is going to be launched to the halo orbit about the Sun-Earth L_2 point in 2018, and the possibility of extending the mission to visit asteroids or planets is currently under discussion. The results of this study will offer the related information of escaping from the L_2 halo orbit.

CIRCULAR RESTRICTED THREE-BODY PROBLEM

Model and Equations of Motion

The *Circular Restricted Three-Body Problem* (CR3BP) assumes a primary and a secondary bodies moving in a circular orbit about their barycenter. The mass of the third body is negligible compared to the masses of the two main bodies. The two main bodies can be the Sun and Earth, the Earth and Moon or etc. The rotating coordinate system with the barycenter at the origin and the main bodies fixed on the x-axis is chosen to describe the motion of the third body (See Figure 1). For convenience, the angular velocity of the rotating frame, the total mass and the distance between the two main bodies are normalized to 1. Thus, the masses of the primary and the secondary bodies, m_1 and m_2, become 1-μ and μ, where μ is the ratio of their masses. The equations of motion are:

$$\ddot{x} - 2\dot{y} = \partial U / \partial x \tag{1}$$

$$\ddot{y} + 2\dot{x} = \partial U / \partial y \tag{2}$$

$$\ddot{z} = \partial U / \partial z \tag{3}$$

where

$$U = \frac{x^2 + y^2}{2} + \frac{(1-\mu)}{r_1} + \frac{\mu}{r_2}$$
$$r_1 = \sqrt{(x+\mu)^2 + y^2 + z^2}$$
$$r_2 = \sqrt{(x-1+\mu)^2 + y^2 + z^2}$$

The system has an energy integral,

$$C = 2U - (\dot{x}^2 + \dot{y}^2 + \dot{z}^2) \tag{4}$$

which is a conserved quantity called *Jacobi integral*.

Equilibrium Points

Reference 10 presents the detail of resolving the equilibrium points from the equations of motion. There are five equilibrium (Lagrange) points, and the three collinear points (L_1, L_2 and L_3) are unstable. The geometries of the five equilibrium points are depicted in Figure 1.

Halo Orbits and Invariant Manifolds

The linearized equations at L_1 and L_2 reveal that there exist periodic orbits about the points. Reference 11 gives the numerical algorithm to find the periodic orbits by making use of the state transition matrix to adjust and finally close the orbit. The halo orbit is the periodic orbit around

L_1, L_2 or L_3 with large out-of-plane (z component) amplitude. As the halo orbits provide constant geometry for observation and communication, besides the historic successful missions, there are several missions being planned to exploit the L_1 and L_2 orbits of the Sun-Earth and Earth-Moon systems. For Sun-Earth system, the period of a halo orbit is around 180 days.

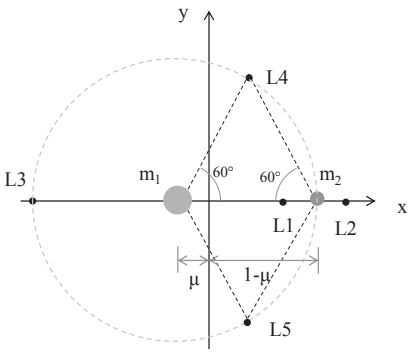

Figure 1. Circular restricted three-body system and Lagrange points.

Table 1. Eigenvalues of the monodromy matrix of the Sun-Earth halo orbit with Az=430000km.

λ_1	λ_2	λ_3	λ_4	λ_5	λ_6
1367	1/1367	0.95+ 0.31i	0.95 - 0.31i	1	1

The state transition matrix (STM) that has mentioned maps the initial state vector (i.e. position and velocity) to the final state vector. It can be acquired by integrating the product of the partial derivative matrix of the state rates and STM. The partial derivative matrix can be acquired based on the equations of motion (Eqs. (1)-(3)). The monodromy matrix is basically the STM for a period of the periodic orbit. We could gain insight about a halo orbit by examining the eigenvalues and eigenvectors of its monodromy matrix. The eigenvalues of the Sun-Earth L_2 halo orbit with z-amplitude, Az=430000km are given in Table 1 for example.

For halo orbits, there are a pair of real eigenvalues (λ_1, λ_2) with $\lambda_1 \cdot \lambda_2=1$, a pair of conjugate complex eigenvalues of modulus 1 (λ_3, λ_4), and two eigenvalues of 1 (λ_5, λ_6).[12] λ_1 is the dominant eigenvalue whose value is around 1500 for the Sun-Earth L_1 and L_2 halo orbits. The eigenvector associated with λ_1 lies in the most diverging direction. Adding a small deviation along that eigenvector to the corresponding initial state vector will efficiently push the spacecraft away from the halo orbit. Such a departure trajectory is referred to the unstable manifold. By propagating the deviations of different magnitudes, one would get the full structure of the unstable manifolds associated to the halo orbit. Figure 2 shows the tube of the unstable manifolds of a halo orbit. On the contrary, backward propagating the deviations along the eigenvector of the eigenvalue smaller than 1 (λ_2) will result in the stable manifolds that naturally converge into the halo orbit.

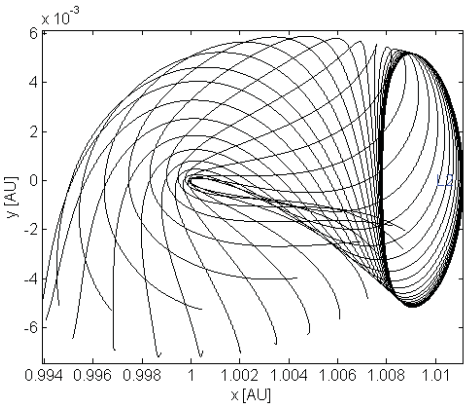

Figure 2. A halo orbit and the associated unstable manifolds.

LUNAR ENCOUNTERS GUIDED BY UNSTABLE MANIFOLDS

Four Cases of Lunar Encounters

Assuming a spacecraft has been in a halo orbit about the L_2 point of the Sun-Earth system, we know a small ΔV can push the spacecraft into an unstable manifold departing from the halo orbit efficiently. Therefore, we are concerned with whether there is any chance that the manifolds encounter with the Moon. The eccentricity and inclination of Moon's orbit are not taken into account. Although it is a simplified model, we could acquire knowledge about the dynamics for mission design. The mission scheme can be refined in a more precise model. It is discovered that the manifold tubes associated with the halo orbits of varied Az generally intersect with Moon's orbit with four crossings of similar geometries. The intersection profiles for the halo orbits of Az=430000km and Az=280000km are depicted in Figure 3. The small circles mark the intersections of manifolds with the ecliptic plane, outlining the intersection lines and showing four intersections with Moon's orbit. Namely, there exist four bunches of manifolds that can encounter with the Moon. The four cases of encounters are numbered in order according to the lunar phases at encounters.

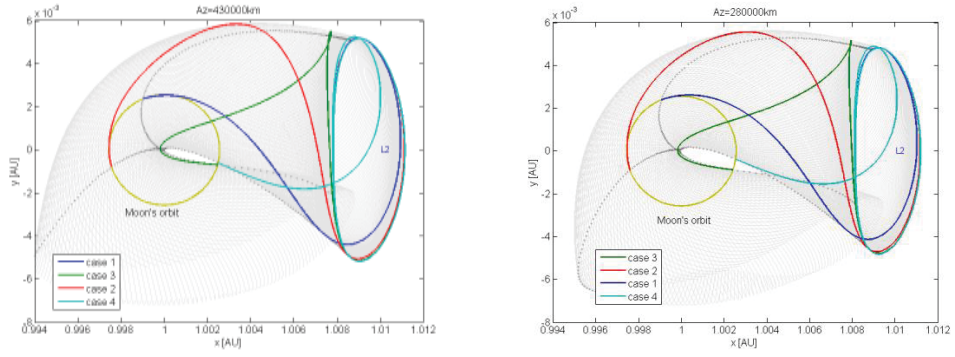

Figure 3. The tubes of unstable manifolds exhibit four intersections with Moon's orbit.

As only negligible magnitudes of deviation were given at the initial point (x=x_{L2}+Ax, y=0, z=Az), the manifolds are of the same Jacobi integral. Besides, as the distances from the encounter points to the Earth are identical and the Sun is relatively far, the velocities of manifolds at lunar encounters should be comparable. However, the V_∞ with respect to the Moon could differ greatly due to different directions approaching the Moon. The trajectories of cases 1 and 2 are shown mostly tangential to Moon's orbit while the cases 3 and 4 are shown mostly perpendicular. Figure 4 shows the V_∞ with respect to the Moon of the four cases as functions of Az. The cases 3 and 4 result in larger V_∞ (around 1.3km/s) as expected. Their V_∞ are nearly equal at any size of halo orbit, which should be due to their similar encounter directions. Moreover, their V_∞ do not vary too much with the size of halo orbit. The cases 1 and 2 result in much smaller V_∞ (around 0.5km/s), which also decay faster as Az decreases.

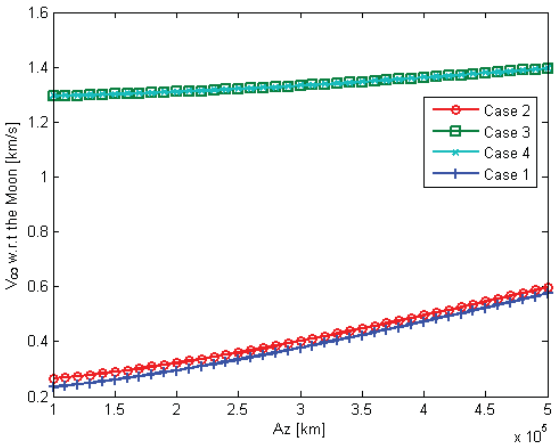

Figure 4. The magnitudes of V_∞ with respect to the Moon as functions of Az.

EFFECTS OF LUNAR SWINGBYS

Evaluation in the 2-body Problem

In the following, the transfers from the halo orbit with Az=430000km are taken as an example for discussion.

Table 2. The C3 (before lunar gravity assists) and ToF of the four cases of lunar encounters.

	Case 1	Case 2	Case 3	Case 4
C_3 (km^2/s^2)	-0.2548	-0.3194	-0.3194	-0.2613
ToF (day)	442.2919	331.7242	363.5857	394.8946

The C_3 (calculated in the 2-body problem) and time of flight (ToF) before lunar swingby for the four encounters are given in Table 2. As the ΔV are basically negligible, the transfers from the halo orbit to lunar encounter can be considered as ballistic flights. The C_3 are comparable and all smaller than 0. With the knowledge of the V_∞ with respect to the Moon, by targeting different

points on the B-plane of lunar swingby, one would get different post-swingby velocities with respect to the Earth. The C_3 after the swingbys are calculated based on the post-swingby velocities. Values of C_3 are displayed along with the corresponding B-planes in Figure 5. The swingbys can lead to both escape and non-escape trajectories. The cases 3 and 4 result in a maximum possible C_3 of $2km^2/s^2$ (V_∞=1.4km/s), which is significant for further interplanetary exploration. The cases 1 and 2 result in a maximum C_3 of 0.2 km^2/s^2. The V_∞ vectors of the escape trajectories are shown in Figure 6. Although cases 3 and 4 result in similar magnitudes of V_∞ with respect to the Moon, the resulting V_∞ with respect to the Earth have opposite distribution for x direction. Because the encounter directions of cases 3 and 4 are nearly opposite, the radius of the Moon exerts different block effects on the trajectory outcomes, as revealed in Figure 5 as well. Both two cases can result in relatively large components in the +y direction, which would lead to a larger heliocentric orbit than Earth's orbit. The small distribution for the –y direction of the cases 1 and 4 indicates smaller heliocentric orbits. The distribution for the +x and –x directions of cases 2 and 4 indicates the possibility of constructing 1:1 resonant orbit with Earth's orbit. For the missions using electric propulsion, such as the DESTINY, a larger V_∞ with respect to the Earth at the second encounter is attainable, which can enhance the flexibility of mission design.

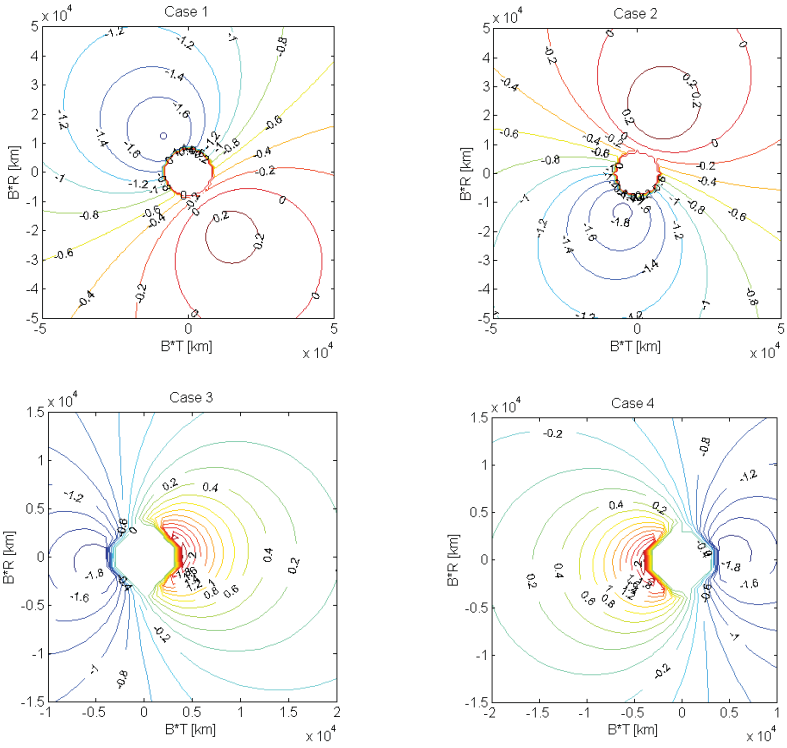

Figure 5. The B-planes for the four cases of lunar swingbys. The contours show the values of the C3 with respect to the Earth after the swingbys.

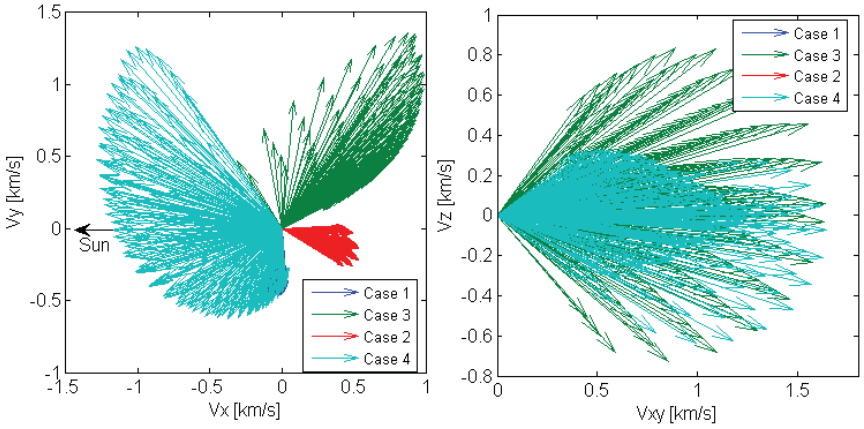

Figure 6. The possible V_∞ with respect to the Earth resulting from the 4 cases of swingbys.

Evaluation in the 3-body Problem

As the 2-body problem neglects the perturbation of the Sun, the swingby effects assessed in that model contain uncertainties. In order to gain more reliable information, the post-swingby trajectories are propagated in the 3-body model. Define the sphere of influence (SoI) of radius= 0.02AU, approximate to two times the Earth-L_2 distance. If the trajectory can reach the SoI, the trajectory is considered to escape; otherwise it is non-escape. Figure 7 shows the propagated trajectories after the swingbys in the 3-body model. The trajectories in black are considered to escape in both 2-body and 3-body problems. The trajectories in red are the escape trajectories that are considered non-escape in the 2-body problem. The trajectories in grey are the non-escape trajectories that are considered to escape in the 2-body problem. As it is revealed, due to the Sun's perturbation, there is actually a larger range of escape trajectories after the lunar swingbys than the 2-body model predicts. The heliocentric orbit period, P and perihelion, r_p of the escape trajectories are plotted in Figure 8. For comparison, the trajectories departing directly via the outward unstable manifolds are also assessed. Figure 9 depicts the direct escape trajectories from the halo orbit. The P and r_p resulting from the direct manifold escapes measured at the SoI are plotted along in Figure 8. The P-rp plots of the escape trajectories via manifolds result in a line. It is known that, in the CR3BP, trajectories comply with an invariant quantity called *Tisserand's criterion*, which is represented as[10]

$$T = r/a + 2[a(1-e^2)/r]^{1/2}\cos i \tag{5}$$

where T is the Tisserand's criterion, r is the distance to the Sun, a is the semi-major axis of the spacecraft, e is the eccentricity and i is the inclination. Because the orbital inclinations of the escape trajectories via manifolds are small, 0.24° at largest, the other two elements are related in a function, which explains the line representing manifold trajectories. It should be noted that, the points of the same P-rp set do not mean the same orbit. Whether to adopt a direct escape from halo orbit or a lunar swingby would depend on the timing and mission requirement. However, undoubtedly, with lunar swingby, we have much more choices of interplanetary orbits to place the spacecraft after a halo orbit mission.

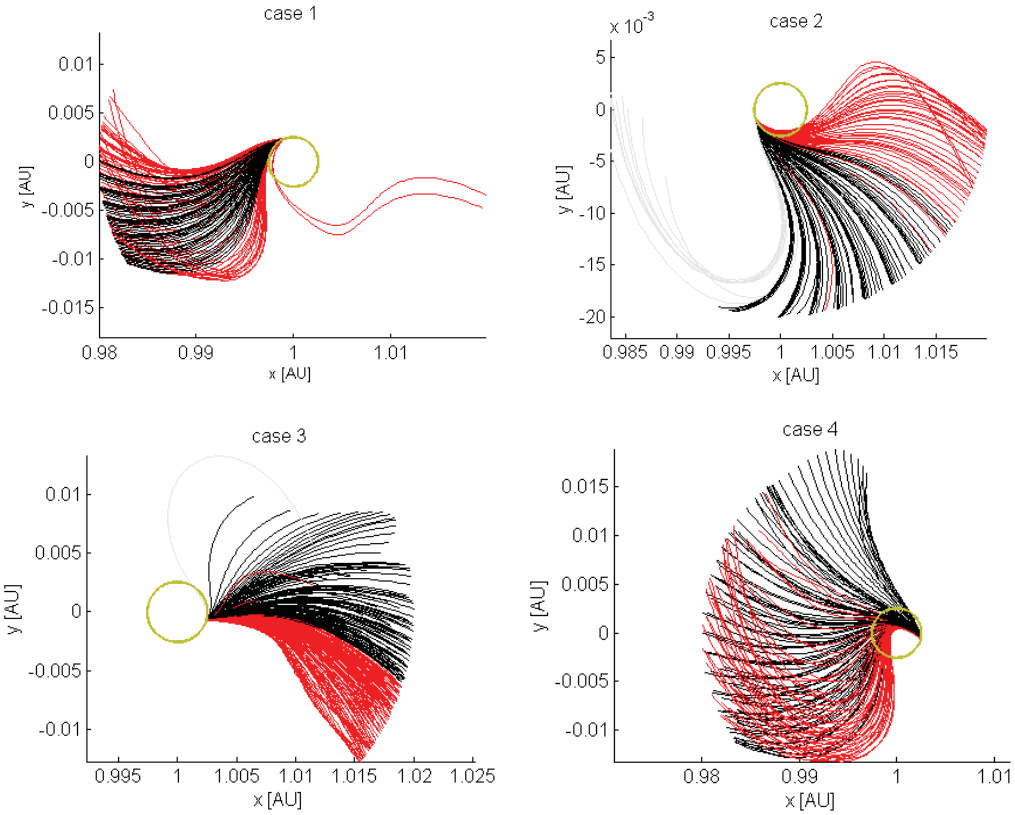

Figure 7. Post-swingby trajectories in the 3-body model.

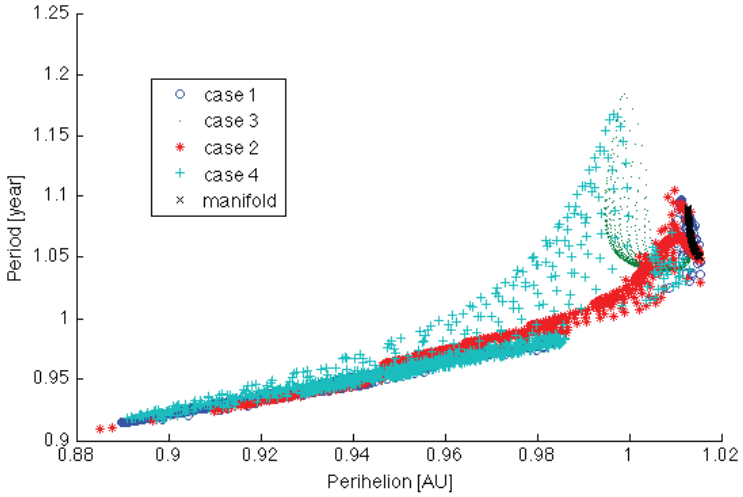

Figure 8. P-rp plot of the escape orbits resulting from lunar swingbys and direct escapes via unstable manifolds.

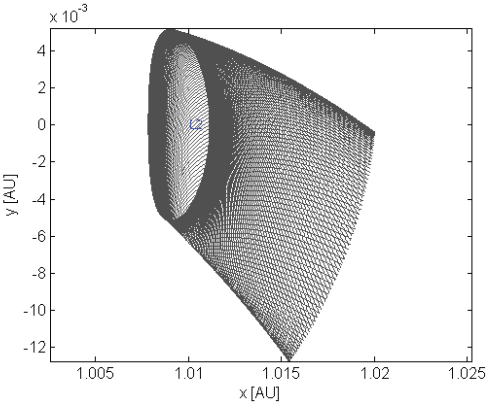

Figure 9. Direct escape trajectories from the halo orbit (outward unstable manifolds).

PHASING PROBLEM

As the structure of manifolds is fixed for the halo orbit of a specified size, the four intersection points and the time of flight (ToF) to the intersection points are also fixed. (Although ToF can be lengthened or shortened by a halo period (≈180 days) by increasing or decreasing the magnitude of deviation by λ_1 times, this way is very limited to adjust the phase of spacecraft with respect to the Moon.) For the above reasons, to make a lunar encounter happen, the requirement on the phase of halo orbit is very strict. Therefore, a phasing maneuver is considered to increase the chance of lunar encounter. This section investigates the required ΔV for the concerned phasing problem.

The problem is depicted in Figure 10. When the spacecraft arrives at one of the four intersections, the Moon is a small phase angle away. By giving some ΔV and meanwhile allowing some difference of ToF, the spacecraft would be able to encounter with the Moon. φ is the phase of the initial encounter, which is fixed for a specified halo orbit, $\Delta\varphi$ is the phase difference between the Moon and the initial encounter, which can be known in an actual application, and ω is the Moon's angular velocity. During the ToF difference Δt, the Moon's phase is changed by $\omega\Delta t$. Therefore, the target phase should be $\varphi+\Delta\varphi+\omega\Delta t$. The correction can be calculated from

$$\delta x_f \cong \Phi \delta x_0 + \frac{\partial x_f}{\partial t}\delta(t) \tag{6}$$

where Φ is the 6x6 STM that maps the state vector (position and velocity) at the maneuver epoch ($\boldsymbol{x_0}$ at t_0) to the state vector at the final epoch ($\boldsymbol{x_f}$ at t_f). Eq. (6) is expanded to

$$\begin{bmatrix} \begin{bmatrix} (\cos(\varphi+\Delta\varphi+\omega\Delta t)-\cos(\varphi))\cdot r_m \\ (\sin(\varphi+\Delta\varphi+\omega\Delta t)-\sin(\varphi))\cdot r_m \\ 0 \end{bmatrix} \\ \Delta\mathbf{v_f} \end{bmatrix} \cong \boldsymbol{\Phi}\begin{bmatrix} \mathbf{0} \\ \Delta\mathbf{v_0} \end{bmatrix} + \begin{bmatrix} \mathbf{v_f} \\ \mathbf{a_f} \end{bmatrix}\Delta t \tag{7}$$

where r_m is the radius of Moon's orbit, $\boldsymbol{v_f}$ and $\boldsymbol{a_f}$ are the velocity and acceleration at final epoch. The difference of velocity at final epoch ($\Delta\boldsymbol{v_f}$) is permitted while the final position should be cor-

rected to the target. Hence, the correction $\Delta\mathbf{v_0}$ can be resolved from the first three linear equations for the known $\Delta\varphi$ and a given Δt. Because it is a linearized equation, the process should be repeated until the final position of the corrected trajectory reaches to the target point. By varying Δt, the minimum ΔV at the maneuver epoch for the given $\Delta\varphi$ can be found.

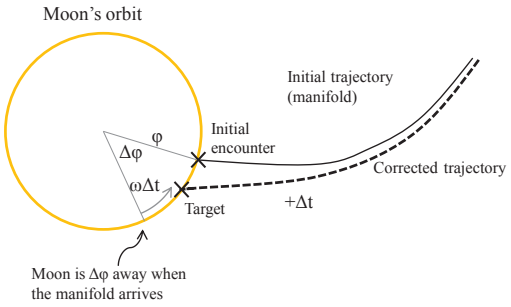

Figure 10. Correcting trajectory to encounter with the Moon.

Table 4. Eigenvalues of the STM that maps velocity at t_f–60d to the position at t_f.

λ_I	λ_{II}	λ_{III}
0.31-0.42i	0.31+0.42i	0.28

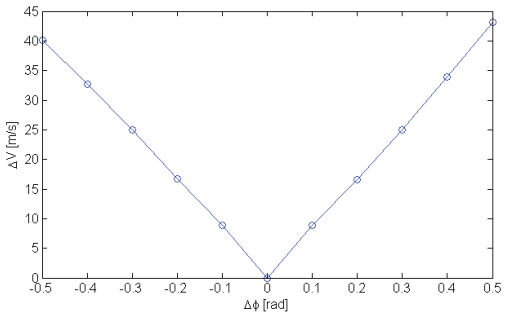

Figure 11. Phasing maneuver ΔV vs Δφ at the t_f-60d epoch for case 3.

As mentioned above, the halo orbit has a greatly dominant eigenvalue (λ_1). If a correction maneuver occurs in or near the halo orbit, a small error due to computer precision or propulsion system will be magnified by λ_1, leading the corrected trajectory far away from the desired trajectory and the linearized dynamics. Therefore, the maneuver is recommended to take place away the portion of halo orbit. Table 4 gives the eigenvalues of the STM that maps the velocity at 60 days before initial encounter to the position at final epoch t_f for case 3. The modulus of the three eigenvalues are comparable, suggesting a maneuver can safely take place at the t_f–60d epoch. Fig-

ure 11 gives the results of minimum ΔV at this epoch for different $\Delta\varphi$. The ΔV profile is nearly symmetric and displays a linear function of $\Delta\varphi$.

The $\Delta\varphi$ can be known in actual application. By examining the minimum required ΔV at different epochs, one would know the best timing to execute a maneuver. Giving a $\Delta\varphi$=–0.5rad, Figure 12 shows the trajectories corrected at different epochs for the four cases. Figure 13 shows the minimum ΔV as functions of maneuver epoch. As it can be seen, the minimum required ΔV are <20m/s for all four cases. According to the symmetry shown in Figure 11, we can suppose a ΔV budget of 20m/s can cover a $\Delta\varphi$ range from –0.5 rad to 0.5 rad, equivalent to a 16% chance for lunar encounter if the halo orbit mission is not pre-phased for a future lunar swingby. According the initial ToF given in Table 2, Figure 14 draws the phases of the Moon should be for each case of encounter when the spacecraft is launched from the initial point of the halo orbit. With a ΔV budget of 20m/s, each phase section for lunar encounter is broadened by 1 rad. The figure indicates a chance of 30% to implement efficient gravity assist (case 3 or 4).

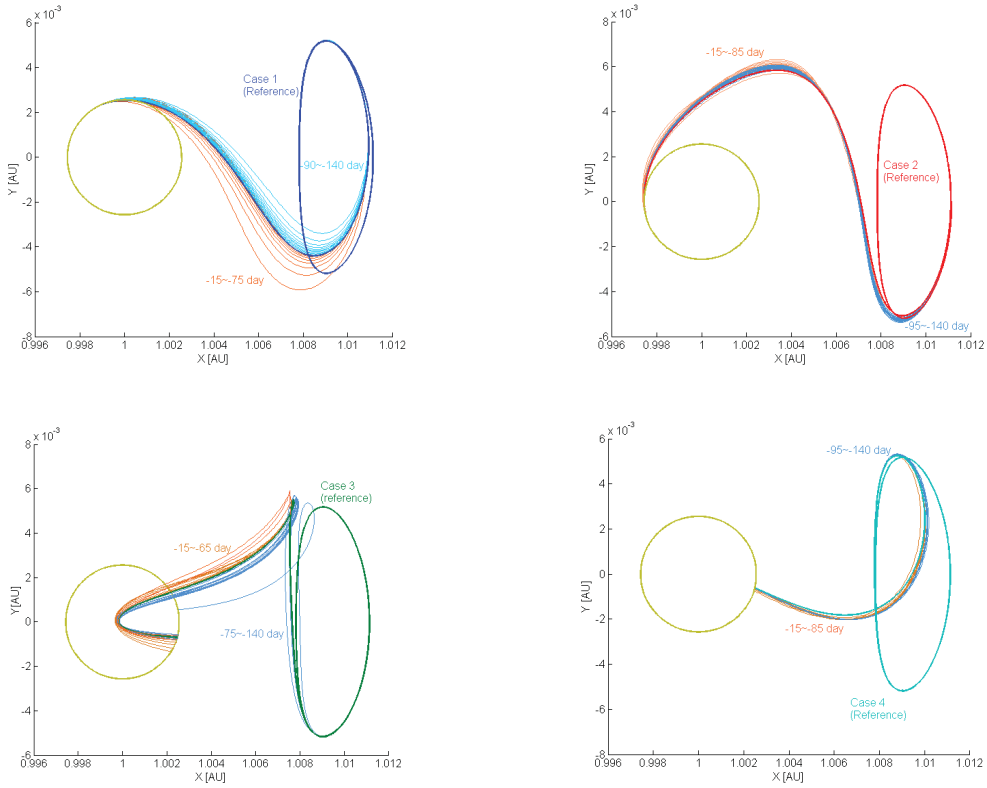

Figure 12. Corrected trajectories to meet the Moon whose phase lags the initial encounter position 0.5 rad.

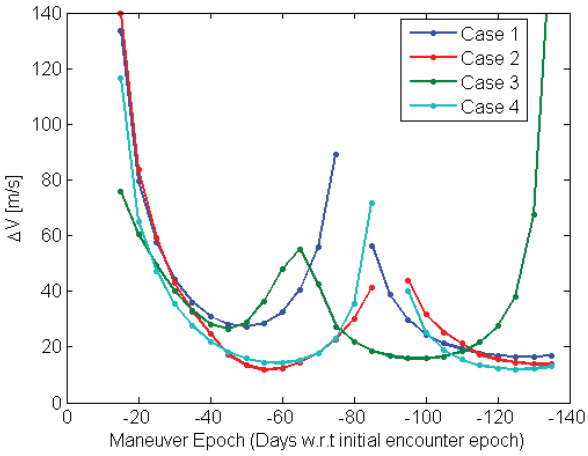

Figure 13. Required minimum correction ΔV at different maneuver epochs.

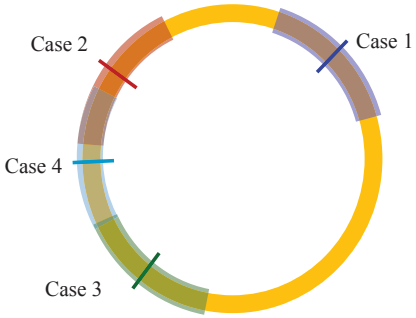

Figure 14. The lunar phases that satisfy the lunar encounter requirements if a ΔV of 20m/s is available.

CONCLUSION

The present study investigates the escape strategy combining unstable manifolds and lunar gravity assist. Results show that

1) There are four cases of lunar encounter guided by the unstable manifolds. Two of the encounter cases can lead to effective gravity assists with a maximum possible C_3 of $2km^2/s^2$;
2) Comparing with the direct escape from the halo orbit, adding a portion of lunar swingby largely broaden the space of orbit choices for an extended mission;
3) With some ΔV budget, the requirements of manifold-guided swingby can be eased to some extent. As calculated, a ΔV of 20m/s can open a chance of 30% for effective gravity assists (case 3 and case 4).

In the future, more compressive analysis can be done regarding the required phasing ΔV to cover full lunar phases and required ΔV for halo orbits of different size. We are also interested in

exploiting the encounters of cases 1 and 2 by an additional lunar swingby to increase V_∞ with respect to the Earth as well as the Moon.

REFERENCES

[1] J.J. Guzman, D.W. Dunham, P.J. Sharer, et al., "Stereo Mission Design Implementation." 20th *International Symposium on Space Flight Dynamics*. Annapolis, Maryland, USA, September 24-28, 2007.

[2] J. Kawaguchi, H. Yamasawa, T. Uesugi and H. Matsuo, "On Making Use of Lunar and Solar Gravity Assists in LUNAR-A, PLANET-B Missions." *Acta Astronautica*. Vol.35, No.9-11, 1995, pp. 633-642.

[3] S. Campagnola, R. Jehn and C. Corral Van Damme, "Design of Lunar Gravity-Assist for the BepiColombo Mission to Mercury." *Advances in the Astronautical Sciences.* Vol. 119, Part I (2004), pp. 427-442.

[4] D. Landau, T.P. McElrath, D. Grebow and N.J. Strange, "Efficient Lunar Gravity Assists for Solar Electric Propulsion Missions." *Advances in the Astronautical Sciences*. Vol. 143, Part I (2012), pp. 917-934.

[5] W.S. Koon, M.W. Lo, J. E. Marsden and S.D. Ross, "Low Energy Transfer to the Moon." *Celestial Mechanics and Dynamical Astronomy*. Vol. 81, 2001, pp. 63-73.

[6] K.C. Howell and M. Kakoi, "Transfers between the Earth-Moon and Sun-Earth Systems Using Manifolds and Transit Orbits." *Acta Astronautica*. Vol. 59, 2006 pp. 367-380.

[7] C. Conley, "Low Energy Transit Orbits in the Restricted Three-body Problem." *Industrial and Applied Mathematics*. Vol. 16, No.4, July 1968, pp. 732-746.

[8] G. Mingotti, F. Topputo and F. Bernelli-Zazzera, "Earth-Mars Transfers with Ballistic Escape and Low-thrust Capture." *Celestial Mechanics and Dynamical Astronomy*. Vol. 110, No. 2, 2011, pp. 169-188.

[10] V. Szebehely, *Theory of Orbits, The Restricted Problem of Three Bodies,* Academic Press, New York and London.

[11] K.C. Howell, "Three-dimensional, Periodic, 'Halo' Orbits." *Celestrial Mechanics*. Vol. 32, 1984, pp.53-71.

[12] W.S. Koon, M.W. Lo, J. E. Marsden and S.D. Ross, *Dynamical systems, the Three-Body Problem and Space Mission Design*, Marsden Books, 2008.